Exploring Robustness in Blood Glucose Control with Unannounced Meal Intake for Type-1 Diabetes Patient

Péter Szalay[1], Dániel András Drexler[2], and Levente Kovács[2]

[1]Elektrobit Automotive Finland Oy, Elektroniikkatie 13, Oulu 90590, Finland, peter.szalay@elektrobit.com
[2]Physiological Controls Research Center, Óbuda University, Bécsi Street 96/B, Budapest 1034, Hungary, kovacs@uni-obuda.hu, drexler.daniel@nik.uni-obuda.hu

Abstract: The importance of efficient diabetes treatment and its' reliable automation is rising with the prevalence of this chronic condition worldwide. Robustness is one of the enablers of the safe automation of plasma glucose control, for it can ensure consistent behavior when the controlled dynamics are changing or partially unknown. Hence, this work focuses on assessing the capabilities of a robust nonlinear controller framework in a simulated environment. Linear Parameter-Varying modeling is combined with robust control techniques, supported by an Unscented Kalman filter. These controllers are then subjected to additional constraints in search of a practical trade-off between disturbance rejection and the severity of transient behavior. Simulations with unannounced meal intakes explore and compare the effect of these additional constraints and configurations using the virtual patients provided by a well-known in silico simulator. The simulation results indicate that this control method can ensure adequate blood glucose control and has the potential to support other control algorithms to realize a safe and reliable artificial pancreas.

Keywords: T1DM; Artificial pancreas; Robust control; LPV; Glycemic controller

1 Introduction

In a healthy individual, a complex endocrine system keeps the glucose concentration in the blood within a narrow range (3.9 - 7.8 [mmol/L]). Diabetes Mellitus (DM) is a collective term referring to several chronic metabolic diseases where this system is impaired, resulting in elevated glucose levels. In particular, Type 1 Diabetes Mellitus (T1DM) is diagnosed when the β-cells in the pancreas cannot produce insulin, a peptide hormone that plays a crucial role in decreasing plasma glucose concentration [1]. The most common treatment for this condition includes regular insulin injections. Due to an increasing prevalence in the population [2, 3], the recent decades saw extensive research in the automation of insulin treatment [4, 5], commonly referred to as Artificial Pancreas (AP). Some

AP implementations have already undergone clinical trials [6–8].

Maintaining normal glucose concentration (normoglycemia) is a challenging control problem due to the following reasons:

- Most models approved for representing a T1DM patient [9–11] are severely nonlinear, even though they focus on only the most relevant aspects of human metabolism.
- Tuning the parameters of these models has practical limitations [12, 13]. Hence, the nominal model can deviate significantly from the actual patient behavior [14, 15].
- The commercially available continuous glucose monitoring (CGM) sensors have significant noise and drift [16–18].
- A single-hormone controller that can only administer insulin has no means to elevate glucose levels. Therefore, the controller must be designed so that the control signal is always non-negative. Controllers with the capability to increase glucose concentration using glucagon [19] is outside the scope of this work due to some practical challenges in glucagon delivery [20].
- Even rapid-acting insulin - if injected subcutaneously - has a significantly slower effect on the plasma glucose concentration than meal intake or physical activity [9, 10].
- The dynamics of the human metabolism concerning glucose is slower when the glucose levels are lower compared to when they are high [21].
- The plasma glucose concentration is affected by various factors that are difficult to measure, detect, or even quantify. These include meal intake, physical activity, insulin administered by the patient (in a semi-automated setting), and various other physiological conditions.
- Having glucose levels below 3.9 mmol/L or 72 mg/dL (hypoglycemia) is a more severe acute complication than high glucose concentration (hyperglycemia). While reducing the latter in severity and frequency is the primary goal of AP, the former can lead to loss of consciousness, seizures, and even death [1] and hence must be strictly avoided [22].

Numerous different approaches were presented for control algorithms [23] that can address the above-listed particularities. These include different incarnations of PID control [24, 25], adaptive controllers [26], machine learning algorithms [27, 28], fractional order controllers [29] among others. One of the most widely accepted approaches is model predictive control (MPC), which showed remarkable results both in simulation and in practice [30, 31]. However, MPC requires an accurate model, which is rarely available in clinical practice. Hence, increasing the robustness of the controllers [32, 33] or making robustness the core feature of the control algorithm [34–36] gained popularity. Despite their limited disturbance rejection capabilities compared to MPC adjusted to individual patients, robust control methods have the potential to achieve a desirable compromise between safety and the efficiency of the T1DM treatment.

This work focuses on a class of robust nonlinear controllers aiming to ensure normoglycemia for T1DM patients. The T1DM model presented in [37] serves as the basis of the controller design, transformed into an LPV model, extended with an output uncertainty model, and weighting functions representing expected tracking performance, reference dynamics, and constraints on the control signal. The LPV controller can ensure robustness by minimizing $\mathscr{H}_\infty$ or $\mathscr{H}_2$ norms between various inputs and outputs of the extended LPV model.

2 Modeling the Human Metabolism

The following differential equations describe the 11th order Cambridge model introduced by Hovorka et al. [9] and later updated by [37]:

$$\begin{aligned}
\dot{C}(t) = \;& -k_{a,int}C(t) + \frac{k_{a,int}}{V_G}Q_1(t) \\
\dot{Q}_1(t) = \;& -\left(\frac{F_{01}}{Q_1(t)+V_G} + x_1(t)\right)Q_1(t) + k_{12}Q_2(t) - \\
& -R_{cl}\max\{0, Q_1(t) - R_{thr}V_G\} - Phy(t) + \\
& +EGP_0\max\{0, 1-x_3(t)\} + \min\left\{U_{G,ceil}, \frac{G_2(t)}{t_{max}}\right\} \\
\dot{Q}_2(t) = \;& x_1(t)Q_1(t) - \Big(k_{12} + x_2(t)\Big)Q_2(t) \\
\dot{x}_1(t) = \;& -k_{b1}x_1(t) + S_{IT}k_{b1}I(t) \\
\dot{x}_2(t) = \;& -k_{b2}x_2(t) + S_{ID}k_{b2}I(t) \\
\dot{x}_3(t) = \;& -k_{b3}x_3(t) + S_{IE}k_{b3}I(t) \\
\dot{I}(t) = \;& \frac{k_a}{V_I}S_2(t) - k_eI(t) \\
\dot{S}_2(t) = \;& -k_aS_2(t) + k_aS_1(t) \\
\dot{S}_1(t) = \;& -k_aS_1(t) + u(t) \\
\dot{G}_2(t) = \;& \frac{G_1(t) - G_2(t)}{t_{abs}(t)} \\
\dot{G}_1(t) = \;& -\frac{G_1(t)}{t_{abs}(t)} + D(t),
\end{aligned} \tag{1}$$

where $C(t)$ is the glucose concentration in the subcutaneous tissue [mmol/L], $Q_1(t)$ and $Q_2(t)$ are the masses of glucose in accessible and non-accessible compartments [mmol], $x_1(t)$ [1/min], $x_2(t)$ [1/min], and $x_3(t)$ [-] are the remote effects of insulin on glucose distribution, disposal and endogenous glucose production, respectively, $I(t)$ is the insulin concentration in plasma [mU/L], $S_1(t)$ and $S_2(t)$ are the insulin masses in the accessible and non-accessible compartments [mU], while $G_1(t)$ and $G_2(t)$ are the masses of ingested glucose in the stomach and gut [mmol/kg]. $u(t)$ is the injected insulin flow of rapid-acting insulin [mU/min], which is the input of the system. $D(t)$ is the amount of ingested carbohydrates [mmol/min], and $Phy(t)$ is the effect of physical activity [mmol/min]. Both are considered as disturbances. Table 1 provides details on model parameters. The glucose absorption time constant $t_{abs(t)}$ is a function of state variables,

Table 1
Cambridge model parameters.

Name	Unit	Description
$k_{a,int}$	1/min	transfer rate constant between the plasma and the subcutaneous compartment
V_G	L	distribution volume of glucose in the accessible compartment
F_{01}	mmol/min	total non-insulin dependent glucose flux
k_{12}	1/min	transfer rate constant from the non-accessible to the accessible compartment
R_{cl}	1/min	renal clearance constant
R_{thr}	mmol/L	glucose threshold for renal clearance
EGP_0	mmol/min	endogenous glucose production extrapolated to the zero insulin concentration
t_{max}	min	time-to-maximum appearance rate of glucose in the accessible compartment
$U_{G,ceil}$	mmol/min/kg	maximum glucose flux from the gut
k_{b1}, k_{b2}	1/min	deactivation rate constants
k_{b3}	1/min	deactivation rate constant for the insulin effect on endogenous glucose production
S_{IT}	L/mU/min	insulin sensitivity for transport
S_{ID}	L/mU/min	insulin sensitivity for distribution
S_{IE}	L/mU	insulin sensitivity for endogenous glucose production
k_a	1/min	insulin absorption rate constant
V_I	L	volume of distribution of rapid-acting insulin
k_e	1/min	fractional elimination rate from plasma

and calculated as follows:

$$t_{abs}(t) = \max\left\{t_{max}, \frac{G_2(t)}{U_{G,ceil}}\right\}. \tag{2}$$

Parameters $k_{a,int}$, F_{01}, k_{12}, EGP_0, k_{b1}, k_{b2}, k_{b3}, S_{IT}, S_{ID}, S_{IE}, k_a and k_e are time-varying with $\pm 5\%$ deviation. In the in silico tests, this is represented by sinusoidal oscillations superimposed on the nominal values with three hour period and a randomly generated phase.

2.1 Model reduction

A high-order model is rather difficult to handle, let it be analysis, identification, observer, or controller design, regardless of the method used. Given the limited measurement capabilities, we can only acquire information from the dominant components of the model dynamics. It would be advantageous to reduce the model to one that retains the most characteristic properties, yet the error resulting from this simplification is minimal. For example, early diabetes models used only three state variables [38], and it is not uncommon in ICU patient models to use only 3-5 state variables [39]. However, the errors resulting from model reduction

must be considered in the controller design.

For the states that belong to meal absorption (which is considered disturbance), it is easy to choose a linear substitution that represents worst-case meal intake. Let us use the notation $W_{meal}(s)$ for the transfer function of this model:

$$W_{meal}(s) = \frac{U_{G,ceil}}{t_{max}s+1}. \tag{3}$$

It is frequent among the most commonly used T1DM models [9, 10, 37, 40, 41] to contain a second-order nonlinear component. In the Cambridge model, these are denoted as $Q_1(t)$ and $Q_2(t)$. Aside from this and the meal absorption, the rest of the dynamics are entirely linear. We can distinguish two main parts: subcutaneous glucose transfer and insulin dynamics. The former can be neglected if an adequate state observer can accurately estimate plasma glucose concentration. The rest incorporates the transfer of the fast-acting insulin from the subcutaneous regions to the plasma, insulin degradation, and insulin effect. The overall model can be simplified by truncating this single input-multiple output linear system.

In the case of (1), the transfer speed between specific compartments is comparable to the sampling time of the CGM. Hence, the states associated with them can be eliminated. The resulting reduced model is as follows:

$$\begin{aligned}
\dot{Q}_1(t) = \; & -\left(\frac{F_{01}}{Q_1(t)+V_G}+x_1(t)\right)Q_1(t)+k_{12}Q_2(t)- \\
& -R_{cl}\max\{0,Q_1(t)-R_{thr}V_G\}-Phy(t)+ \\
& +EGP_0\max\left\{0,1-\frac{k_aS_{IE}}{V_Ik_e}S_2(t)\right\}+\min\left\{U_{G,ceil},\frac{G_2(t)}{t_{max}}\right\} \\
\dot{Q}_2(t) = \; & x_1(t)Q_1(t)-\left(k_{12}+\frac{k_aS_{ID}}{V_Ik_e}S_2(t)\right)Q_2(t) \\
\dot{x}_1(t) = \; & k_{b1}\left(\frac{k_aS_{IT}}{V_Ik_e}S_2(t)-x_1(t)\right) \\
\dot{S}_2(t) = \; & -k_aS_2(t)+k_aS_1(t) \\
\dot{S}_1(t) = \; & -k_aS_1(t)+u(t) \\
\dot{G}_2(t) = \; & \frac{G_1(t)-G_2(t)}{t_{abs}(t)} \\
\dot{G}_1(t) = \; & -\frac{G_1(t)}{t_{abs}(t)}+D(t)
\end{aligned} \tag{4}$$

where the output is $C(t) \approx Q_1(t)/V_G$.

Finally, considering the range of parameter k_{12} as presented in [37], if $1/k_{12}$ is comparable to the CGM sensor sample time, then there is a need to apply reduction in the nonlinear dynamics as well. Section 3.1 provides details on how to perform the necessary changes.

3 Controller Synthesis

3.1 Linear Parameter-Varying representation

Although continuous time T1DM models can have a varying degree of nonlinearity, the vast majority of them can be transformed into a linear parameter-varying model: [42]

$$\begin{array}{c} \dot{\mathrm{x}}(t) = \mathbf{A}(\rho(t))\mathrm{x}(t) + \mathbf{B}(\rho(t))\mathrm{u}(t) \\ \mathrm{y}(t) = \mathbf{C}(\rho(t))\mathrm{x}(t) + \mathbf{D}(\rho(t))\mathrm{u}(t) \\ \mathbf{A}(\rho(t)) = \mathbf{A}_0 + \sum_{i=1}^{m} \rho_i(t)\mathbf{A}_i \quad \mathbf{B}(\rho(t)) = \mathbf{B}_0 + \sum_{i=1}^{m} \rho_i(t)\mathbf{B}_i \\ \mathbf{C}(\rho(t)) = \mathbf{C}_0 + \sum_{i=1}^{m} \rho_i(t)\mathbf{C}_i \quad \mathbf{D}(\rho(t)) = \mathbf{D}_0 + \sum_{i=1}^{m} \rho_i(t)\mathbf{D}_i, \end{array} \tag{5}$$

where the scheduling variables $\rho_i(t)$ are bounded, as well as their time derivatives, and these bounds are known. Furthermore, the scheduling variables should be available for measurement. For a T1DM model, the bound constraint is satisfied, but only estimation of the scheduling variables is available.

The chosen LPV representation of the Cambridge model is the following:

$$\begin{aligned} \dot{C}(t) = & \; -k_{a,int}C(t) + \frac{k_{a,int}}{V_G}Q_1(t) \\ \dot{Q}_1(t) = & \; -\left(F_a\rho_1(t) + F_b\right)Q_1(t) - \rho_1(t)x_1(t) + k_{12}Q_2(t) - dist_{Rcl}(t) - \\ & -Phy(t) + EGP_0\left(1 - x_3(t)\right) + \frac{U_{G,ceil}}{t_{max}}\tilde{G}(t) \\ \dot{Q}_2(t) = & \; \rho_1(t)x_1(t) - k_{12}Q_2(t) - \rho_2(t)x_2(t) \\ \dot{x}_1(t) = & \; -k_{b1}x_1(t) + S_{IT}k_{b1}I(t) \\ \dot{x}_2(t) = & \; -k_{b2}x_2(t) + S_{ID}k_{b2}I(t) \\ \dot{x}_3(t) = & \; -k_{b3}x_3(t) + S_{IE}k_{b3}I(t) \\ \dot{I}(t) = & \; \frac{k_a}{V_I}S_2(t) - k_eI(t) \\ \dot{S}_2(t) = & \; -k_aS_2(t) + k_aS_1(t) \\ \dot{S}_1(t) = & \; -k_aS_1(t) + u(t) \\ \dot{\tilde{G}}(t) = & \; -\frac{1}{t_{max}}\tilde{G}(t) + dist_{meal}(t), \end{aligned} \tag{6}$$

which is constructed with the following considerations. The state variables Q_1 and Q_2 were chosen as scheduling variables: $\rho_1 = Q_1$ and $\rho_2 = Q_2$. The Hill function $F_{01}(Q_1(t)+V_G)^{-1}$ has a linear approximation $F_a\rho_1(t)+F_b$, as presented in [43] and [44]. The worst-case meal model (3) replaces the second-order meal intake. Moreover, to avoid switching control, endogenous glucose production (EGP) has no saturation, and the renal extraction (R_{cl}) is considered a disturbance: $dist_{Rcl}(t)$. In exchange, the controller must ensure that $x_3(t) <= 1$.

If model reduction is necessary, the same method is applicable as presented in Section 2.1. In addition, if $1/k_{12}$ is comparable to the CGM sensor sample time, then further model reduction is possible by replacing $Q_1(t)$ and $Q_2(t)$ with $\tilde{Q}(t) \approx Q_t(t) - x_1(t)/k_{12}$ as follows:

$$\begin{aligned}\dot{C}(t) = &\quad -k_{a,int}C(t) + \frac{k_{a,int}}{V_G}\tilde{Q}(t) - \frac{k_{a,int}}{k_{12}V_G}x_1(t)\\ \dot{\tilde{Q}}(t) = &\quad -(F_a\rho_1(t)+F_b)\tilde{Q}(t) + (F_c\rho_1(t)+F_d)x_1(t) - dist_{Rcl}(t) -\\ &\quad -Phy(t) - \rho_2(t)x_2(t) + EGP_0(1-x_3(t)) + \frac{U_{G,ceil}}{t_{max}}\tilde{G}(t),\end{aligned} \tag{7}$$

where we used the approximation $F_c\rho_1(t)+F_d \approx Q_1(t)F_{01}/(k_{12}(Q_1(t)+V_G))$. Furthermore, the output can be approximated with

$$C(t) \approx \frac{1}{V_G}\left(\tilde{Q}(t) - \frac{1}{k_{12}}x_1(t)\right), \tag{8}$$

if necessary.

Note, that even though $Q_1(t)$ and $Q_2(t)$ are not part of the model (7), the scheduling variables $\rho_1(t)$ and $\rho_2(t)$ are still present, hence the state observer must provide reliable estimation, and cannot use (7) instead of (1).

Considering the nonlinearity of the Cambridge model and the presence of disturbances, sigma-point filters are good candidates for estimating the scheduling variables [45–47]. These filters provide further benefits of reducing the measurement noise of CGMS, estimating the glucose flux from unannounced meal intakes, as well as enabling state feedback control.

The state observer used in this work is the same as presented in [43], i.e., we use unscented square-root filter with lognormal distribution for state variables associated with glucose concentration and meal intake.

3.2 Modeling Uncertainties

Not even one of the most complex T1DM models [48] can fully capture a system as complex as human metabolism. All models used in practice employ some level of simplification, capturing only the most essential aspects of the glucose-insulin interaction. Additionally, human physiology tends to change and adapt over time and is affected by various external factors that are difficult to quantify, let alone measure [49, 50]. No matter the model used, controller design must address deviation from the actual dynamics. This approach uses uncertainty weighting functions to that end. Let P denote a nominal T1DM model, with a single output $y(t)$, a single controlled input $u(t)$, and a set of external disturbances $\mathrm{d}(t)$. Figure 1 presents a simple system that uses output uncertainty weighting functions.

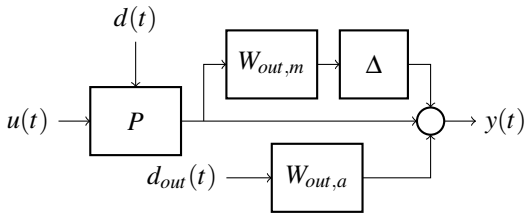

Figure 1
Simple system with output uncertainty weighting functions

$W_{out,a}$ and $W_{out,m}$ are linear minimum-phase systems representing additive and multiplicative output uncertainty, respectively. Δ is an unknown linear system that is of minimum-phase and has an $\mathscr{H}_\infty$-norm that is less or equal to 1. $d_{in}(t)$ and $d_{out}(t)$ are considered stochastic disturbance signals, that are usually modeled with distribution $\mathscr{N}(0,1)$ or $\mathscr{U}(-1,1)$.

There are other ways to model uncertainties, but this work only considers output uncertainties. The parameters of $W_{out,a}$ and $W_{out,m}$ may come from the residual error of fitting T1DM parameters or from a priori knowledge from clinical practice. Here the uncertainty model accounts for the sinusoidal changes in model parameters presented in section 2, and any reduction ((7) and section 2.1) that may take place.

Extending the nominal model with uncertainties is vital for both the controller and state observer, as it can ensure robustness and stability for both control and state estimation. However, it also poses a challenge if the control law is realized with state feedback. In this particular case, the state variables of the uncertainty models shall be estimated as well.

3.3 LPV Model in the Clinical Practice

Before presenting the controller synthesis, it is worth examining the LPV transformed model from a different perspective. In (7), in the subsystem consisting of $Q_1(t)$ and $Q_2(t)$, $\rho_1(t)$ defines the rate of transfer of glucose from $Q_1(t)$ to $Q_2(t)$ compartments, and $\rho_2(t)$ is responsible for how fast glucose in $Q_2(t)$ dissipates from the system. Since $\rho_1(t)$ is identical to $Q_1(t)$, and the output is $\approx Q_1(t)/V_G$, hence the larger the glucose levels are, the faster the dynamics of the system. This is a common observation in clinical practice as well.

Consequently, this poses a challenge to controller design: Suppose the controller injects too much insulin during hyperglycemia. In that case, it is difficult to compensate for its effect once the glucose levels decrease, not only because negative control signal is not an option but also because the system will be less sensitive to any intervention.

3.4 Robust Controller Synthesis

In order to address the need for robustness and stability, $\mathscr{H}_\infty$ and hybrid $\mathscr{H}_\infty/\mathscr{H}_2$ controllers [51] can provide a solid foundation. Let $\mathbf{G}(j\omega,\rho)$ denote the transfer matrix of an LPV (5) closed-loop system with an $\mathscr{H}_\infty$ controller, that was successfully synthesized for a positive γ value. This controller ensures that $\|\mathbf{G}\|_\infty$, the $\mathscr{H}_\infty$ norm of the transfer matrix is smaller than γ:

$$\|\mathbf{G}\|_\infty = \sup_{\rho} \sup_{\omega\in\mathbb{R}} \sigma_{max}(\mathbf{G}(j\omega,\rho)) < \gamma, \tag{9}$$

where σ denotes the singular value. An $\mathscr{H}_2$ controller on the other hand ensures that $\|\mathbf{G}\|_2$, the $\mathscr{H}_\infty$ norm of the transfer matrix is smaller than γ:

$$\|\mathbf{G}\|_2 = \sup_{\rho} \sqrt{\frac{1}{2\pi} trace \int_{-\infty}^{\infty} \mathbf{G}(j\omega, \sup_{\rho})(\mathbf{G}(j\omega, \sup_{\rho}))^H d\omega} < \gamma. \tag{10}$$

$\mathscr{H}_\infty$ and $\mathscr{H}_2$ constraints can be imposed on the controlled system with carefully chosen linear matrix inequalities (LMIs) [52].

Figure 2 and Figure 3 display two different schemes: LPV state feedback, denoted with $K_{fb}(\rho)$, and dynamic LPV controller, denoted with $K_d(\rho)$.

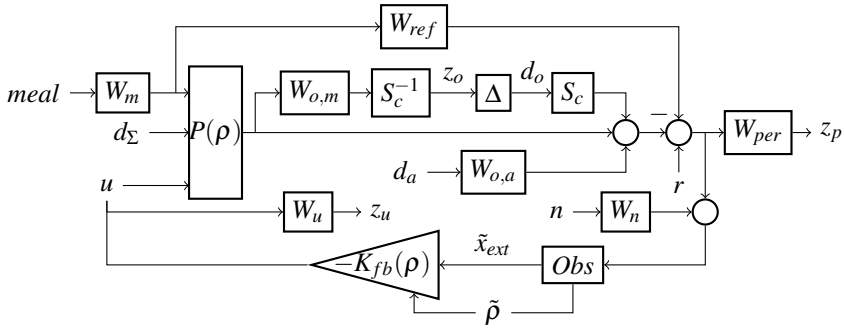

Figure 2
Controller realized as LPV state feedback

$P(\rho)$ represents the LPV transformed T1DM model (6) with reduction applied if necessary, and the meal absorption dynamics separated into W_m. *Obs* denote the sigma point filter that provides state variable ($\tilde{x}_{ext}$) and scheduling variable estimation ($\tilde{\rho}$). $W_{o,m}$ and $W_{a,m}$ are weighting functions for multiplicative and additive output uncertainty models, respectively, with the latter driven by d_a. W_{per} defines expected tracking performance. W_u serves two purposes:

1. it defines the maximum value for the control signal;
2. it ensures that endogenous glucose production does not saturate.

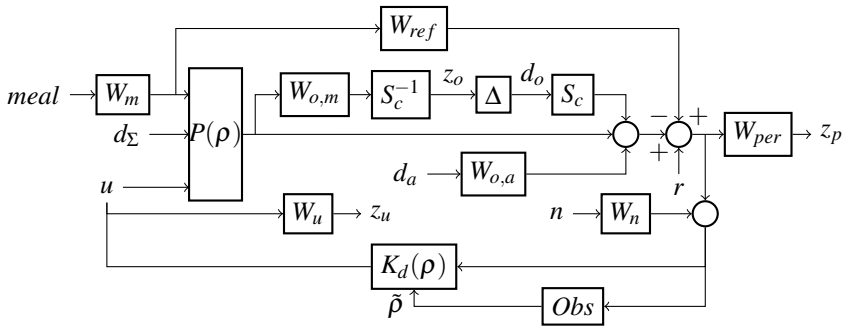

Figure 3
Controller realized as dynamic LPV system

d_Σ represents all disturbance signals affecting $P(\rho)$ directly: *Phy* physical activity, the estimation error of glucose flux from the gut, and quantization error if the control signal has a finite resolution. Since an estimated output of W_m is available, it is possible to define reference tracking dynamics W_{ref} that mimics the behavior of a healthy patient. Using the output of W_{ref} instead of relying on a constant reference signal r for feedback can potentially help avoid hypoglycemia. Finally, W_n noise model is not present for state feedback control.

The state observer works with (1) instead of (6), and will use $W_{o,m}$, $W_{a,m}$, and W_n regardless of the control method used. Section 3.5 details the role of scaling factor S_c.

Pure $\mathscr{H}_\infty$ controller will ensure minimal $\mathscr{H}_\infty$ norm for the transfer to the performance output z_p and smaller than 1 $\mathscr{H}_\infty$ norm to z_o and z_u from the disturbance inputs *meal*, d_a, d_o, d_Σ and n. The latter ensures robust stability for the controlled system. Hybrid $\mathscr{H}_\infty/\mathscr{H}_2$ controller minimizes the $\mathscr{H}_2$ norm for the performance output instead of $\mathscr{H}_\infty$ norm.

Finally, additional LMI constraints limit the poles of the controlled system to a defined region, reducing oscillatory transients and rejecting poles too fast compared to the sampling frequency of the CGM sensor (Figure 4).

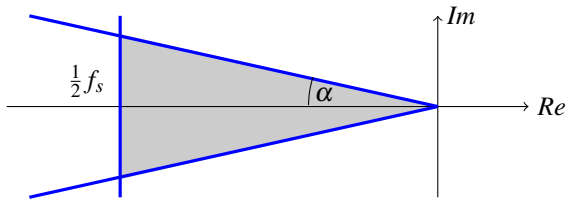

Figure 4
Constraints for the poles of the controlled system: f_s is the sampling frequency of the CGM sensor, α is the maximum angle of the complex conjugate pole pairs

The control law for LPV state feedback is as follows:

$$u(t) = -\mathrm{K}_{fb}(\rho(t))\tilde{x}_e xt(t), \tag{11}$$

where $\tilde{x}_{ext}(t)$ is the estimated state variables of $P(\rho)$, W_m, W_u, $W_{o,m}$, $W_{o,a}$, W_{ref}, and W_{per}.

If the controller is a dynamic LPV system (5) instead, the control signal is the output of the following:

$$\begin{array}{rl} \dot{\mathrm{x}}_d(t) & = \mathbf{A}_d(\rho(t))\mathrm{x}_d(t) + \mathrm{B}_d(\rho(t))e(t) \\ u(t) & = \mathrm{C}_d(\rho(t))\mathrm{x}_d(t) + D_d(\rho(t))e(t). \end{array} \tag{12}$$

3.5 Scaling

In order to achieve robust stability, the $\mathscr{H}_\infty$ norm of the transfer function from the disturbance inputs to the output of W_u and $W_{out,m}$ shall be smaller than 1. On the other hand, the glucose levels can reach up to 17 mmol/L, even with a well-functioning artificial pancreas.

Hence, when using the multiplicative output uncertainty model, the output of the corresponding weighting function (z_o in Figure 2 and Figure 3) should be scaled (S_c) to satisfy robust stability constraints. If S_c is too small, the controller synthesis is infeasible. Conversely, too large scaling factor will lead to reduced disturbance rejection performance. In this work, we used an iterative algorithm to set a patient-specific scaling factor.

4 Results

All simulations were performed on the original eight patient parameter sets introduced in [37]. The weighting functions presented in Figure 2 and Figure 3 are as follows:

- $P(\rho)$ is the LPV-transformed model (6), with patient-specific reduction applied only to remove state variables that would otherwise introduce time constants less than 20 minutes.
- Transfer function (3) is chosen as W_m in Figure 2 and Figure 3, using patient-specific parameters.
- $W_{o,m}$ is a low pass filter that represents 10% to 25% multiplicative uncertainty on frequencies below $\frac{2\pi}{120}$ [rad/min]:

  $$W_{o,m}(s) = \frac{0.1}{120s+1} \tag{13}$$

  The higher uncertainty value is necessary when working with a linear model and controller instead of LPV.

- $W_{o,a}$ assume ± 0.5 [mmol/L] additive uncertainty on top of the multiplicative uncertainty.
- W_u is patient-specific, ensuring that endogenous glucose production does not reach zero and that u is smaller than 4500 [mU/min].
- The sensor noise is assumed to be Gaussian white noise with 0.1 [mmol/L] standard deviation, hence $n \approx \mathcal{N}(0,1)$ and $W_n = 0.1$.
- W_{per} specifies that the controller should only minimize tracking error below $\frac{2\pi}{180}$ [rad/min]:

$$W_{per}(s) = \frac{1}{180s+1} \tag{14}$$

- If applicable, the reference dynamics W_{ref} is:

$$W_{ref}(s) = \frac{11}{U_{G,ceil}(60s+1)} \tag{15}$$

  The constant reference signal is 4.5 [mmol/L] and 4.9 [mmol/L] with and without W_{ref} respectively.

We used MATLAB and SIMULINK for controller synthesis and simulation, including the CVX toolbox [53, 54]. For each controller, $\alpha = 45^\circ$ and 5 minutes sampling time constrain the closed-loop poles as shown in (Fig. 4).

For easier comparison with other methods, the simulations were done using two commonly used meal intake scenarios spanning 24 hours. The controller administered the insulin without manual intervention and any meal intake announcement. The meal intake scenarios were as follows:

1. 150 g of carbohydrate (CHO) intake per day. The meal intake consists of a 35 g CHO breakfast at 8:30, a 65 g CHO lunch at 13:00, and a 50 g CHO dinner at 19:00.
2. The meal intake protocol is presented in [55]. It consists of a 45 g CHO breakfast at 9:30, a 75 g CHO lunch at 13:30, and an 85 g CHO dinner at 19:30.

Control variability grid analysis (CVGA) [55] visualizes and compares the capabilities of different types of controller configurations on Figure 5, Figure 6, Figure 7, and Figure 8. The x and y axis is the minimum and maximum glucose levels throughout the simulations, respectively, in [mg/dL]. The aim is to stay in the A and B zones for both meal scenarios for all virtual patients. In each figure, two sets of simulation results are presented: black circles represent simulations using a state feedback controller. In contrast, the simulations result when a dynamic LPV controller was applied are represented with white circles.

Figure 5 displays the CVGA of simulations results for linear $\mathscr{H}_\infty$ controllers, without reference dynamics W_{ref}. The output multiplicative uncertainty is 25%, as ensured by (13). Both the state feedback and the dynamic controller performed poorly, reaching only C and D zones with the majority of virtual patients.

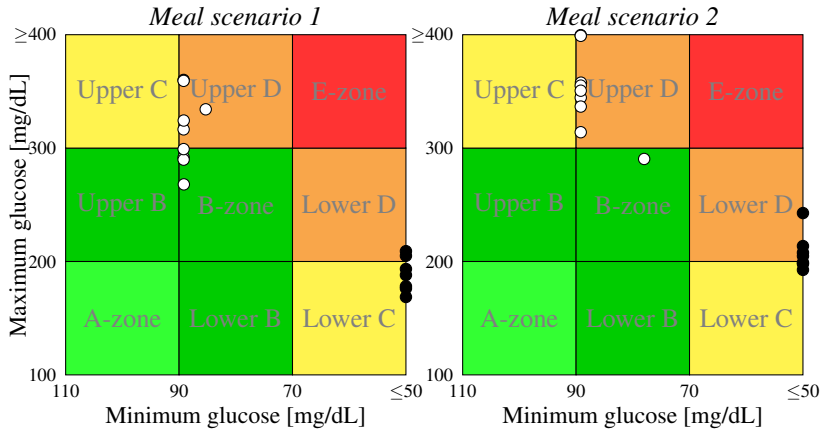

Figure 5
CVGA for linear $\mathscr{H}_\infty$ controllers using (**a**) meal scenario 1 and (**b**) meal scenario 2.

Since the linearization of the model was at 4.9 [mmol/L] ($\approx$ 90 [mg/dL]), both controllers assume slow dynamics, which does not hold once the glucose levels elevate after each meal intake. However, the behavior of the two controller configurations is different. The state feedback controller administers more insulin than necessary, leading to lower maximum values but severe hypoglycemia. In contrast, the dynamic controller avoids hypoglycemia at the cost of higher maximum glucose levels.

Choosing a different working point with a higher glucose level for linearization could improve the capabilities of both controllers. Furthermore, using hybrid $\mathscr{H}_\infty/\mathscr{H}_2$ norm or reference tracking dynamics can bring some minor improvement. However, using a purely linear controller has its limits, and hence a nonlinear approach is necessary.

Using LPV model and LPV controllers reduce the occurrence of both hypo- and hyperglycemia, as shown in Figure 6. Since the controllers directly address the changing dynamics of the model, more than half of the virtual patients are kept in the B-zone for both controller types.

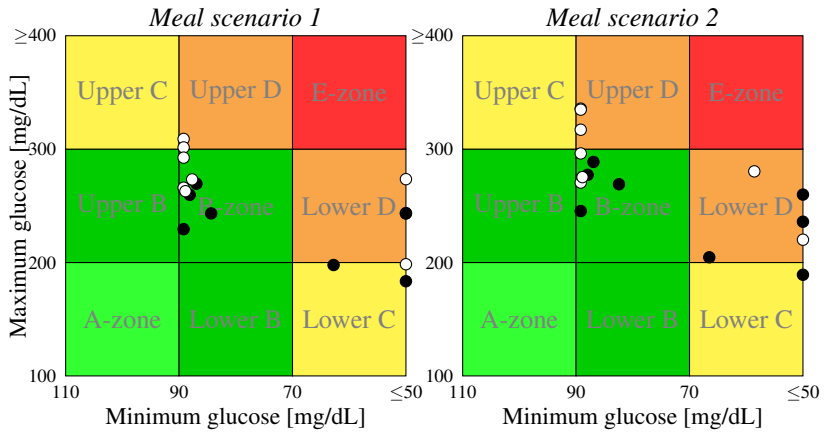

Figure 6
CVGA for LPV $\mathscr{H}_\infty$ controllers using (**a**) meal scenario 1 and (**b**) meal scenario 2.

However, there are cases of severely low glucose concentrations for both controller types. Introducing reference tracking dynamics can mitigate these hypoglycemic episodes, as shown in Figure 7. Instead of a constant reference signal at 4.9 [mmol/L], the additional weighting function $W_{ref}(s)$ defines the desired disturbance rejection. The input of $W_{ref}(s)$ is the estimated glucose flux resulting from meal intake. Both the occurrence and severity of hypoglycemia decreased for the two types of controllers compared to Figure 6, although they are not eliminated completely. The maximum glucose concentration is below 300 [md/dL] for the state feedback controller but increased for the dynamic controller.

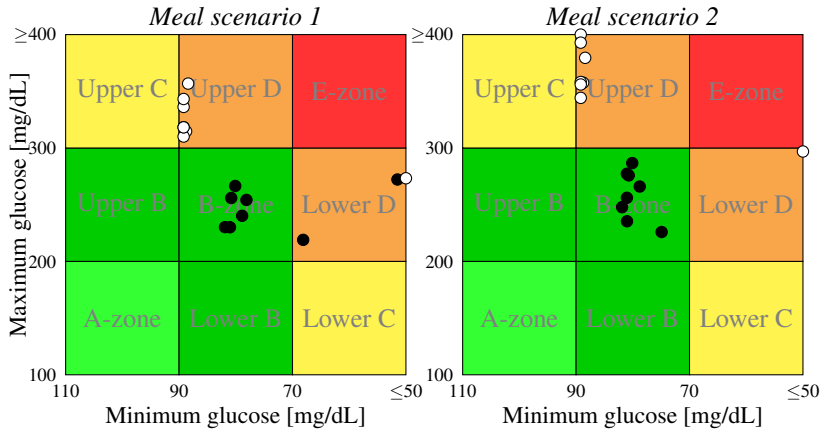

Figure 7
CVGA for state-feedback and dynamic controllers using reference tracking dynamics W_{ref} for (**a**) meal scenario 1 and (**b**) meal scenario 2.

Finally, the results can be further improved by using $\mathscr{H}_2$ norm for the performance output instead of $\mathscr{H}_\infty$. The results are displayed in Figure 8. As a result, the minimum glucose values in both meal scenarios and controller types have less variance and hence lessen the chance of hypoglycemia.

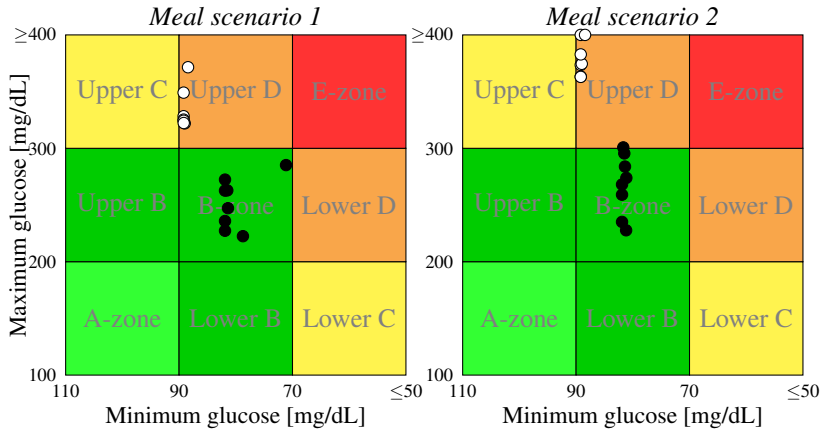

Figure 8
CVGA for LPV $\mathscr{H}_\infty/\mathscr{H}_2$ controllers with W_{ref} using (**a**) meal scenario 1 and (**b**) meal scenario 2.

Conclusions

Based on the simulation results presented in section 4, a linear controller is insufficient for glycemic control. LPV controllers are more reliable than linear ones, with less variability in both maximum and minimum glucose levels for the used meal intake protocols. However, they are still prone to hypoglycemia. Using reference tracking dynamics instead of a constant reference signal can considerably lessen both the occurrence and the severity of these events without compromising the severity of hyperglycemia. Moreover, using a hybrid norm for controller synthesis: $\mathscr{H}_\infty$ for stability and $\mathscr{H}_2$ for performance can provide further benefits. Generalized $\mathscr{H}_2$ and $\mathscr{L}_1$ norm [52] was not in the scope of this work. However, there is a significant difference between using state feedback or a dynamic controller, even though the combination of a sigma point filter and an LPV state feedback is technically a dynamic controller as well. Using the same constraints and extended model, the resulting dynamic controller will lead to higher minimum and maximum glucose levels in the CVGA compared to a state feedback controller. The reason is that the transfer function of the former across all scheduling variables is akin to a high pass filter. Therefore, it will compensate low frequency tracking errors poorly. Introducing an integrator [51] to eliminate this error will result in an infeasible convex synthesis problem.

Even though the presented results may be satisfactory, there are still limitations that must be addressed in future works. LPV model can represent most of the nonlinearity present in the Cambridge model, but it does not capture the positive nature of the system. All the measures to avoid hypoglycemia only indirectly

addressed the constraint that the control signal is non-negative. Despite the parameter variability in the Cambridge model, changes in insulin sensitivity or using different types of insulin are not part of it. Furthermore, a robust controller combined with an accurate meal and fault detection [56] can increase both performance and safety [49, 50]. Finally, a crucial next step is to incorporate the detection of unannounced physical activity. One potential approach is to use the model presented by Resalat et al. [57] is an extension of the Cambridge model that includes a dynamic physical activity subsystem. Early prediction of potential hypoglycemic episodes is necessary since a single hormone system cannot raise the plasma glucose concentration.

Further work shall address the limitations mentioned above and perform validation with the UVA/PADOVA simulator, which is approved by the U.S. Food and Drug Administration (FDA) as an alternative to animal testing of Type 1 diabetes control strategies [11].

Acknowledgment

Project no. 2019-1.3.1-KK-2019-00007. has been implemented with the support provided from the National Research, Development and Innovation Fund of Hungary, financed under the 2019-1.3.1-KK funding scheme. This project has been supported by the Hungarian National Research, Development and Innovation Fund of Hungary, financed under the TKP2021-NKTA-36 funding scheme.

References

[1] A. Fonyo and E. Ligeti. *Physiology*. Medicina, Budapest, third edition, 2008.

[2] S. Wild, G. Roglic, A. Green, R. Sicree, and H. King. Global prevalence of diabetes. Estimates for the year 2000 and projections for 2030. *Diabetes Care*, 27(5):1047–1053, 2004.

[3] R. Buzzetti, S. Zampetti, and P. Pozzilli. Impact of obesity on the increasing incidence of type 1 diabetes. *Diabetes, obesity & metabolism*, 22(7):1009–1013, 2020.

[4] H. Thabit and R. Hovorka. Coming of age: the artificial pancreas for type 1 diabetes. *Diabetologia*, 59(9):1795–1805, 2016.

[5] J. Tašić, M. Takács, and L. Kovács. Control engineering methods for blood glucose levels regulation. *Acta Polytechnica Hungarica*, 19:127–152, 08 2022.

[6] J. Kropff and J. H. DeVries. Continuous glucose monitoring, future products, and update on worldwide artificial pancreas projects. *Diabetes Technology & Therapeutics*, 18(S2), 2016.

[7] G. Forlenza, S. Deshpande, T. Ly, D. Howsmon, F. Cameron, N. Baysal, E. Mauritzen, T. Marcal, L. Towers, B. Bequette, L. Huyett, J. Pinsker, R. Gondhalekar, F. Doyle, D. Maahs, B. Buckingham, and E. Dassau. Application of zone model predictive control artificial pancreas during extended use of infusion set and sensor: A randomized crossover-controlled home-use trial. *Diabetes Care*, 40:dc170500, 06 2017.

[8] P. Colmegna, F. Garelli, H. De Battista, F. Bianchi, and R. S. Sánchez-Peña. The arg algorithm: clinical trials in Argentina. In R. S. Sánchez-Peña and D. R. Cherñavvsky, editors, *The Artificial Pancreas*, pages 79–104. Academic Press, 2019.

[9] R. Hovorka, V. Canonico, L. Chassin, U. Haueter, M. Massi-Benedetti, M. O. Federici, T. Pieber, H. Schaller, L. Schaupp, T. Vering, and M. Wilinska. Nonlinear model predictive control of glucose concentration in subjects with type 1 diabetes. *Physiological measurement*, 25:905–920, 2004.

[10] L. Magni, D. M. Raimondo, C. D. Man, G. D. Nicolao, B. Kovatchev, and C. Cobelli. Model predictive control of glucose concentration in type 1 diabetic patients: An in silico trial. *Biomedical Signal Processing and Control*, pages 338–346, 2009.

[11] C. D. Man, F. Micheletto, D. Lv, M. Breton, B. Kovatchev, and C. Cobelli. The UVA/PADOVA type 1 diabetes simulator: New features. *Journal of Diabetes Science and Technology*, 8(1):26–34, 2014.

[12] H. Kirchsteiger, S. Pölzer, R. Johansson, E. Renard, and L. del Re. Direct continuous time system identification of MISO transfer function models applied to type 1 diabetes. *In Proc. of 50th IEEE CDC-ECC Conference, Orlando, USA*, pages 5176–5181, 2011.

[13] G. Eigner, K. Koppány, P. Pausits, and L. Kovács. Nonlinear identification of glucose absorption related to diabetes mellitus. In *2017 IEEE 21st International Conference on Intelligent Engineering Systems (INES)*, pages 265–270, 2017.

[14] L. Kovács and P. Szalay. Uncertainties and modeling errors of type 1 diabetes models. *Prediction Methods for Blood Glucose Concentration: Design, Use and Evaluation*, pages 211–225, 2016.

[15] R. Blanc, H. M. R. Ugalde, P.-Y. Benhamou, G. Charpentier, S. Franc, E. Huneker, E. Villeneuve, and M. Doron. Modeling the variability of insulin sensitivity for people with type 1 diabetes based on clinical data from an artificial pancreas study. In *2019 41st Annual International Conference of the IEEE Engineering in Medicine and Biology Society (EMBC)*, pages 5465–5468, 2019.

[16] T. Battelino and J. Bolinder. Clinical use of real-time continuous glucose monitoring. *Current Diabetes Reviews*, 4:218–222, 2008.

[17] A. Facchinetti, S. Del Favero, G. Sparacino, J. R. Castle, W. K. Ward, and C. Cobelli. Modeling the glucose sensor error. *IEEE Transactions on Biomedical Engineering*, 61(3):620–629, 2014.

[18] M. Vettoretti, G. Cappon, G. Acciaroli, A. Facchinetti, and G. Sparacino. Continuous glucose monitoring: Current use in diabetes management and possible future applications. *Journal of Diabetes Science and Technology*, 12(5):1064–1071, 2018.

[19] M. Infante, D. A. Baidal, M. R. Rickels, A. Fabbri, J. S. Skyler, R. Alejandro, and C. Ricordi. Dual-hormone artificial pancreas for management of type 1 diabetes: Recent progress and future directions. *Artificial Organs*, 45(9):968–986, 2021.

[20] L. M. Wilson and J. R. Castle. Stable liquid glucagon: Beyond emergency hypoglycemia rescue. *Journal of Diabetes Science and Technology*, 12(4):847–853, 2018. PMID: 29415555.

[21] M. Somogyi and M. Kirstein. Insulin as a cause of extreme hyperglycemia and instability. *Weekly Bulletin of the St Louis Medical Society*, 32:498–510, 1938.

[22] T. Mohammadridha, P. Rivadeneira, N. Magdelaine, M. Cardelli, and C. Moog. Positively invariant sets of a t1dm model: Hypoglycemia prediction and avoidance. *Journal of the Franklin Institute*, 356, 05 2019.

[23] S. Mehmood, I. Ahmad, H. Arif, U. Ammara, and A. Majeed. Artificial pancreas control strategies used for type 1 diabetes control and treatment: A comprehensive analysis. *Applied System Innovation*, 3:31, 07 2020.

[24] F. Shmarov, N. Paoletti, E. Bartocci, S. Lin, S. A. Smolka, and P. Zuliani. Smt-based synthesis of safe and robust pid controllers for stochastic hybrid systems. In O. Strichman and R. Tzoref-Brill, editors, *Hardware and Software: Verification and Testing*, pages 131–146, Cham, 2017. Springer International Publishing.

[25] D. Calupiña, A. García, O. Camacho, A. Rosales, and P. Rivadeneira. Nonlinear PID and dynamic SMC for the artificial pancreas control in the treatment of type 1 diabetes. In *2018 IEEE Third Ecuador Technical Chapters Meeting (ETCM)*, pages 1–6, 2018.

[26] K. Turksoy and A. Cinar. Adaptive control of artificial pancreas systems - a review. *Journal of Healthcare Engineering*, 5, 2014.

[27] T. Zhu, K. Li, P. Herrero, and P. Georgiou. Basal glucose control in type 1 diabetes using deep reinforcement learning: An in silico validation. *IEEE Journal of Biomedical and Health Informatics*, 25(4):1223–1232, 04 2021.

[28] J. C. Peiró. Comparing artificial pancreas controlled by hybrid "closed-loop" machine learning (ML) trained algorithm to multi-daily injection (MDI), insulin pump without CGM and "sensor assisted" insulin pump therapies for diabetes type 1 (DT1) treatment. In *Proceedings of the 2020 International Conference on Data Analytics for Business and Industry: Way Towards a Sustainable Economy (ICDABI)*, pages 1–6, 2020.

[29] A. Mohammadzadeh and T. Kumbasar. A new fractional-order general type-2 fuzzy predictive control system and its application for glucose level regulation. *Applied Soft Computing*, 91:106241, 2020.

[30] B. Kovatchev, C. Cobelli, and E. Renard. Multi-national study of subcutaneous model-predictive closed-loop control in type 1 diabetes: summary of the results. *Journal of Diabetes Science and Technology*, 4:1374–1381, 2010.

[31] D. Shi, E. Dassau, and F. J. Doyle III. Multivariate learning framework for long-term adaptation in the artificial pancreas. *Bioengineering & Translational Medicine*, 4(1):61–74, 2019.

[32] D. Boiroux, M. Hagdrup, Z. Mahmoudi, K. Poulsen, H. Madsen, and J. B. Jørgensen. An ensemble nonlinear model predictive control algorithm in an artificial pancreas for people with type 1 diabetes. In *Proceedings of the 2016 European Control Conference (ECC)*, pages 2115–2120, 2016.

[33] N. Paoletti, K. S. Liu, H. Chen, S. Smolka, and S. Lin. Data-driven robust control for a closed-loop artificial pancreas. *IEEE/ACM Transactions on Computational Biology and Bioinformatics*, 17(6):1981–1993, 11 2020.

[34] R. Parker, F. Doyle, J. Ward, and N. Peppas. Robust $\mathscr{H}_\infty$ glucose control in diabetes using a physiological model. *American Institute of Chemical Engineers*, 46(12):2537–2549, 2000.

[35] G. Rigatos, P. Siano, and A. Melkikh. A nonlinear optimal control approach of insulin infusion for blood glucose levels regulation. *Intellectual Industrial Systems*, 3(2):91–102, 11 2017.

[36] A. Mirzaee, M. Dehghani, and M. Mohammadi. Robust LPV control design for blood glucose regulation considering daily life factors. *Biomedical Signal Processing and Control*, 57:101830, 2020.

[37] M. Wilinska, L. Chassin, C. Acerini, J. Allen, D. Dunger, and R. Hovorka. Simulation environment to evaluate closed-loop insulin delivery systems in type 1 diabetes. *Journal of diabetes science and technology*, 4(1):132–144, 2010.

[38] R. Bergman, L. Phillips, and C. Cobelli. Physiological evaluation of factors controlling glucose tolerance in man. *Journal of Clinical Investigation*, 68:1456–1467, 1981.

[39] J. G. Chase, B. Benyo, and T. Desaive. Glycemic control in the intensive care unit: A control systems perspective. *Annual Reviews in Control*, 48:359–368, 2019.

[40] C. Dalla Man, R. Rizza, and C. Cobelli. Meal simulation model of the glucose-insulin system. *IEEE Transactions on Biomedical Engineering*, 54(10):1740–1749, 2007.

[41] P. Colmegna and R. Sánchez-Peña. Analysis of three T1DM simulation models for evaluating robust closed-loop controllers. *Computer methods and programs in biomedicine*, 113, 10 2013.

[42] F. Bianchi, M. Moscoso-Vásquez, P. Colmegna, and R. Sánchez-Peña. Invalidation and low-order model set for artificial pancreas robust control design. *Journal of Process Control*, 76:133–140, 02 2019.

[43] P. Szalay, Z. Benyó, and L. Kovács. Long-term prediction for T1DM model during state-feedback control. In *Proceedings of the 2016 12th IEEE International Conference on Control and Automation (ICCA)*, pages 311–316, 2016.

[44] P. Szalay, G. Eigner, and L. A. Kovács. Linear matrix inequality-based robust controller design for type-1 diabetes model. *Proceedings of the 19th IFAC World Congress*, 47(3):9247–9252, 2014. 19th IFAC World Congress.

[45] D. Boiroux, T. B. Aradóttir, M. Hagdrup, N. K. Poulsen, H. Madsen, and J. B. Jørgensen. A bolus calculator based on continuous-discrete unscented kalman filtering for type 1 diabetics. *IFAC Papers Online*, 48(20):159–164, 2015. 9th IFAC Symposium on Biological and Medical Systems BMS 2015.

[46] Z. Mahmoudi, K. Nørgaard, N. K. Poulsen, H. Madsen, and J. B. Jørgensen. Fault and meal detection by redundant continuous glucose monitors and the

unscented Kalman filter. *Biomedical Signal Processing and Control*, 38:86–99, 2017.

[47] E. Aguirre-Zapata, J. Cardenas-Cartagena, and J. Garcia-Tirado. Glycemic monitoring in critical care using nonlinear state estimators. *Proceedings of the 20th IFAC World Congress*, 50(1):4430–4435, 2017.

[48] J. Sorensen. *A Physiologic Model of Glucose Metabolism in Man and its Use to Design and Assess Improved Insulin Therapies for Diabetes*. PhD thesis, Massachusetts Institute of Technology, 1985.

[49] K. Turksoy, S. Samadi, J. Feng, E. Littlejohn, L. Quinn, and A. Cinar. Meal detection in patients with type 1 diabetes: A new module for the multivariable adaptive artificial pancreas control system. *IEEE Journal of Biomedical and Health Informatics*, 20(1):47–54, 2016.

[50] L. Meneghetti, A. Facchinetti, and S. D. Favero. Model-based detection and classification of insulin pump faults and missed meal announcements in artificial pancreas systems for type 1 diabetes therapy. *IEEE Transactions on Biomedical Engineering*, 68(1):170–180, 2021.

[51] K. Zhou. *Robust and Optimal Control*. Prentice Hall, New Jersey, 1996.

[52] C. Scherer and S. Weiland. *Linear Matrix Inequalities in Control*. Lecture Notes, Delft Center for Systems and Control, Delft, The Netherlands, 2004.

[53] M. Grant and S. Boyd. CVX: Matlab software for disciplined convex programming, version 2.1. `http://cvxr.com/cvx`, 03 2014.

[54] M. Grant and S. Boyd. Graph implementations for nonsmooth convex programs. In V. Blondel, S. Boyd, and H. Kimura, editors, *Recent Advances in Learning and Control*, Lecture Notes in Control and Information Sciences, pages 95–110. Springer-Verlag Limited, 2008. `http://stanford.edu/~boyd/graph_dcp.html`.

[55] L. Magni, D. Raimondo, C. D. Man, M. Breton, S. Patek, G. D. Nicolao, C. Cobelli, and B. Kovatchev. Evaluating the efficacy of closed-loop glucose regulation via control-variability grid analysis. *Journal of diabetes science and technology*, 2(4):630–635, 2008.

[56] L. Pokorádi, S. Koçak, and E. T'oth-Laufer. Fuzzy failure modes and effects analysis using summative defuzzification methods. *Acta Polytechnica Hungarica*, 18(9):111–126, 2021.

[57] N. Resalat, J. Youssef, R. Reddy, and P. Jacobs. Design of a dual-hormone model predictive control for artificial pancreas with exercise model. In *Proceedings of 2016 38th Annual International Conference of the IEEE Engineering in Medicine and Biology Society, EMBC 2016*, Proceedings of the Annual International Conference of the IEEE Engineering in Medicine and Biology Society, EMBS, pages 2270–2273. Institute of Electrical and Electronics Engineers Inc., October 2016.